

DECAY SCHEME OF  $\text{Te}^{131m}$ 

A. BĂDESCU, O. M. KALINKINA, K. P. MITROFANOV, A. A. SOROKIN, N. V. FORAFONTOV, and V. S. SHPINEL'

Institute of Nuclear Physics, Moscow State University

Submitted to JETP editor August 7, 1960

J. Exptl. Theoret. Phys. (U.S.S.R.) **40**, 91-100 (January, 1961)

The  $\gamma$  and  $\beta$  radiation accompanying the decay of the  $\text{Te}^{131m}$  isomer ( $T_{1/2} = 30$  hr) was measured with a scintillation  $\gamma$  coincidence spectrometer, a two-lens  $\beta$  spectrometer and a  $\beta\gamma$ -coincidence spectrometer. A decay scheme for the decay of the  $\text{Te}^{131m}$  nucleus is proposed. Levels at 0.15, 0.60, 0.78, 0.92, 1.62, 1.82, 1.92, 2.00, and 2.24 Mev have been established for the daughter nucleus  $\text{I}^{131}$ . The spins and parities of a number of levels have been determined from the data on the multipolarities and relative intensities of the  $\gamma$  and  $\beta$  transitions.

## INTRODUCTION

THE present work is a continuation of the investigations of the decay scheme of the  $\text{Te}^{131}$  nucleus ( $T_{1/2} = 30$  hr), the preliminary results of which have been published previously.<sup>1</sup> One can also find in reference 1 a brief survey of other work devoted to the decay of this isotope. In reference 1, we made an accurate determination of the  $\gamma$  spectrum and established the excited levels of the  $\text{I}^{131}$  nucleus with energies of 147, 595, 780, and 2200 keV. It was shown there that the  $\text{I}^{131}$  level scheme presented by Hebb<sup>2</sup> is inaccurate. However, the results were not sufficiently complete to determine the positions of the levels lying between the 780- and 2200-keV levels. In the present work, the measurements were made under better conditions than previously. First, for the preparation of the source we used 99.9%  $\text{Te}^{130}$ -enriched tellurium. (The methods of eliminating the daughter isotope  $\text{I}^{131}$  from the source and of obtaining the samples have been described previously.<sup>1</sup>) Second, for the measurements of the  $\gamma\gamma$  coincidences, we used NaI(Tl) crystals of large size and recorded the spectra with the aid of a 100-channel pulse-height analyzer of type AI-100. Moreover, the partial  $\beta$  spectra were separated by the method of  $\beta\gamma$  coincidences. All this made it possible to obtain more complete information on the  $\text{Te}^{131m}$  decay scheme.

 $\gamma$  SPECTRUM

After removal of the  $\text{I}^{131}$  isotope from the sample, we measured the  $\gamma$ -ray spectrum of  $\text{Te}^{131m}$  on a scintillation spectrometer. For the measurement of the hard  $\gamma$  rays ( $E_\gamma > 400$  keV) we used

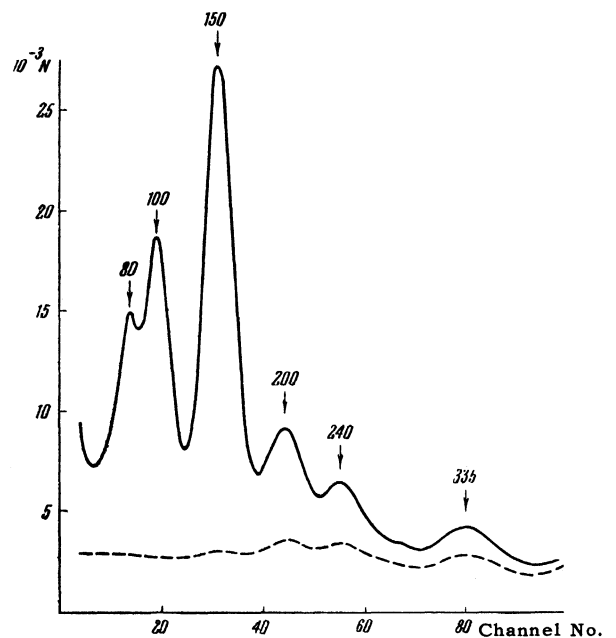


FIG. 1.  $\gamma$  spectrum of  $\text{Te}^{131m}$  in the energy region up to 400 keV. The spectrum measured with a 2 mm Pb + 0.5 mm Cd filter is indicated by the dotted line. This makes it possible to take into account the contribution from the Compton distributions of the harder  $\gamma$  transitions. In this figure and in subsequent figures, the energies in keV are shown above the peaks.

a  $40 \times 40$  mm NaI(Tl) crystal with a resolving power of 10% on the 660-keV  $\text{Cs}^{137}$  line. The soft region of the spectrum was measured with a crystal of diameter 30 mm and height 14 mm, having a better resolving power (8.5%). Figure 1 shows the  $\gamma$ -ray spectrum in the low-energy region below 400 keV. The  $\gamma$ -ray spectrum in the high-energy region (to 2500 keV) has been given previously.<sup>1</sup>

Table I  
Energy and Intensities of  $\text{Te}^{131\text{m}}$   $\gamma$  Lines

Scintillation spectrometer	$E_\gamma$ , keV		$I_\gamma$ , % (scintillation spectrometer)
	Photoelectron spectrum	Conversion-electron spectrum	
80±5	—	81±0,5	5±1
100±5	101±1	101,5±0,5	8±2
150±5	149±2	149±1	25±5
—	183±2	182±0.2	—
200±5	201±3	—	~8
240±5	240±5	241±5	~4
—	—	277±5	—
335±5	333±5	330±5	18±6
450±10	~454	~454	12±3
590±10	~588	—	~4
780±10	780±5	780±5	100
850±15	840±10	840±10	50±10
920±20	925±10	—	14±5
1080±20	—	—	6±2
1140±20	1140±15	—	27±5
1220±20	1220±15	—	20±5
1350±30	—	—	~2
1540±30	—	—	~1,5
1650±30	—	—	3±1
1920±30	—	—	2,5±0,5
2000±30	—	—	4,6±0,5
2240±30	—	—	0,94±0,2

In the present experiment we determined more accurately the energy of some hard lines and made a more careful resolution of the spectrum. The energies ( $E_\gamma$ ) and intensities ( $I_\gamma$ ) of the  $\gamma$  rays obtained from these measurements are shown in Table I. Columns 2 and 3 of this table give the  $\gamma$ -transition energies obtained from the photoelectron and internal-conversion electron spectra, respectively, measured on a two-lens  $\beta$  spectrometer. The spectrum of the photoelectrons were measured

with lead radiators of 8-mm diameter and thicknesses of 11 mg/cm<sup>2</sup> and 4 mg/cm<sup>2</sup>. The half-width of the lines was 4%. The intensities of the  $\gamma$  transitions in the energy region > 700 keV obtained from the photoelectron spectrum are in agreement with the data of the scintillation  $\gamma$  spectrum. In the softer region the determination of the intensities from the photoelectron lines was not carried out, owing to the large Compton background from hard  $\gamma$  rays.

FIG. 2. Conversion-electron (I—Current in spectrometer coils).

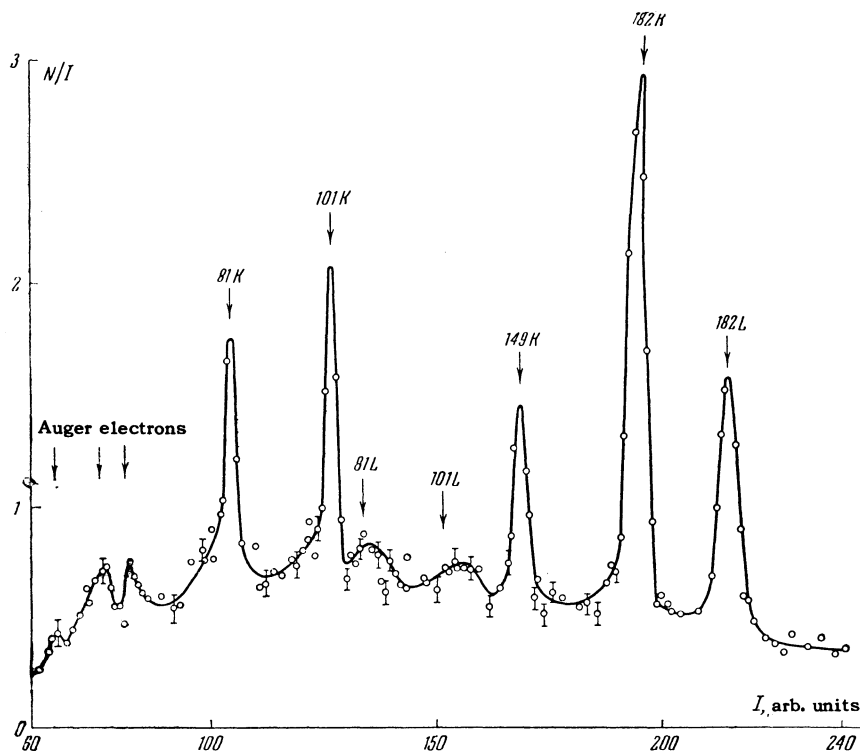


**Table II**  
**Internal-Conversion Coefficients for  $\gamma$  Transitions**

$E_{\gamma}$ , keV	$\alpha_K$	$\alpha_K / \alpha_L$	Theoretical value of $\alpha_K$			Proposed multipolarity
			E2	M1	E1	
81±0.5	2.06±0.45	$\geq 5$	2.3	1.2	0.3	M1+ E2
101.5±0.5	1.23±0.28	$\geq 5$	1.12	0.603	0.166	M1+ E2
149±1	0.26±0.05	—	0.3	0.195	0.05	M1+ (E2)

### CONVERSION-ELECTRON SPECTRUM

The conversion-electron spectrum in the 10–200 keV region measured on a two-lens  $\beta$  spectrometer is shown in Fig. 2. A source  $\sim 0.1$  mg/cm<sup>2</sup> thick was used in the measurements of this spectrum. The thickness of the counter window was  $\sim 0.1$  mg/cm<sup>2</sup> and its transmission threshold was 8 keV. The resolving power of the spectrometer in these measurements was 2%. The intensity ratio of the 81-, 101.5-, and 149-keV conversion lines can be determined from the spectrum. Using the ratio of intensities corresponding to the  $\gamma$  lines in the  $\gamma$  spectrum and the value of the conversion coefficient  $\alpha_K = 0.26 \pm 0.05$  for the 149-keV transition obtained by Sorokin,<sup>3</sup> we can obtain the value of  $\alpha_K$  for the 81- and 101.5-keV transitions. Moreover, we can estimate for these transitions the value of the ratio  $\alpha_K/\alpha_L$ . These data are shown in Table II, which also gives the theoretical values of  $\alpha_K$  for various multiplicities. Comparison of our data for  $\alpha_K$  with the theoretical values indicates that the 81- and 101.5-keV transitions can be of the M1 or E2 type, or a mixture of both, but the large value of the ratio  $\alpha_K/\alpha_L$  ( $\geq 5$ ) indicates that in all probability they are preferentially of the M1 type with a possible admixture of E2.

Also visible in the spectrum shown in Fig. 2 are the intense K and L peaks from the 182-keV  $\gamma$  transition occurring in  $\text{Te}^{131}$  (isomeric transition of the M4 type). Apart from the peaks shown in Fig. 2, peaks from  $\gamma$ -rays of energies 24, 277, 330, 780, and 840 keV were also visible in the spectrum. In reference 1, the coefficient  $\alpha_K$  for the 780-keV transition was determined from a comparison of the intensities of the conversion and photoelectron lines from the 780-keV  $\gamma$  transition in  $\text{I}^{131}$  with the intensities of the corresponding lines from the 364-keV  $\gamma$  transition in  $\text{Xe}^{131}$  ( $\text{I}^{131}$  was not separated from the sample), whose conversion coefficient  $\alpha_K$  is known. It turned out to be  $(0.8 \pm 0.2) \times 10^{-3}$  and corresponded to a transition of the E1 type.

In the present work we repeated these measurements by a somewhat different method. We pre-

pared sources of  $\text{Te}^{131}$  and  $\text{Cs}^{137}$  and, under identical geometrical conditions, we measured the relative intensities of the conversion lines on a  $\beta$  spectrometer and of the  $\gamma$  lines with a scintillation spectrometer. The coefficient  $\alpha_K$  for the 662-keV transition in  $\text{Ba}^{137}$  is known well<sup>4</sup> and the conversion coefficient for the 780-keV transition can be determined from the expression

$$\alpha_{K780} = \alpha_{K662} (I_{\gamma662}/I_{\gamma780}) (I_{e780}/I_{e662}).$$

These measurements gave the value  $\alpha_{K780} = (1 \pm 0.3) \times 10^{-3}$ , in agreement with the value obtained by us previously and with the multipolarity ascribed to this transition. The conversion coefficient for the 840-keV transition was not specifically determined, but, by using the available experimental data, we could estimate it to be  $\sim 2 \times 10^{-3}$ , which is also in agreement with the previously<sup>1</sup> reported value  $(1.6 \pm 0.6) \times 10^{-3}$  and corresponds to the multipole orders M1, E2, or a mixture of both.

### BETA SPECTRUM

The  $\beta$  spectrum was measured on a two-lens  $\beta$  spectrometer with a source thickness of 1 mg/cm<sup>2</sup>, resolving power of  $\sim 4\%$ , and a transmission of  $\sim 5\%$ . A Fermi plot was made of the spectrum and the partial  $\beta$  spectra were separated (Fig. 3). In subtracting the hardest spectrum ( $E_{\text{max}} = 2460$  keV), which was a unique spectrum ( $\Delta J = 2$ , yes)<sup>2</sup>, we introduced a correction factor of the form

$$a_1(W) = (W^2 - 1) + (W_0 - W)^2.$$

The spectrum was not resolved in the soft-energy region ( $< 300$  keV). The shape of the spectrum in this region indicates the existence of a component with  $E_{\text{max}} \approx 200$  keV. This was confirmed by measurements based on the  $\beta\gamma$ -coincidence method. All the data on the  $\text{Te}^{131}$   $\beta$  spectra are shown in Table III. In this table, the energies of the soft components are taken from the measurements of the partial  $\beta$  spectra by the  $\beta\gamma$ -coincidence method. Apart from the  $\beta$  spectra shown in Table III, we observed a spectrum with  $E_{\text{max}} = 690 \pm 40$  keV and intensity  $\sim 6.5\%$  of the full

Table III  
 $\beta$  spectra of  $\text{Te}^{131}$

$E_{\beta\text{max}}$ , keV	Relative intensity, %			log $ft$
	Full $\beta$ spectrum	$\beta$ -spectra of isomer with $T_{1/2}=25$ min	$\beta$ spectra of isomer with $T_{1/2}=30$ hr	
2457 $\pm$ 10	3.76 $\pm$ 0.4	—	3.76 $\pm$ 0.4	9.45
2150 $\pm$ 20	7.85 $\pm$ 0.8	42.3 $\pm$ 4	—	6.81
1680 $\pm$ 50	3 $\pm$ 0.3	16.2 $\pm$ 2	—	6.30
1365 $\pm$ 25	7.67 $\pm$ 0.8	41.4 $\pm$ 4	—	5.54
570 $\pm$ 30	30.9 $\pm$ 3	—	30.9 $\pm$ 3	6.15
420 $\pm$ 30	43.4 $\pm$ 4	—	43.4 $\pm$ 4	5.56
215 $\pm$ 15	3.6	—	3.6	5.69

spectra. It can be assumed that it is associated with the decay of  $\text{Te}^{127}$ , a small admixture of which could have been contained in our sample. An intensive  $\beta$  spectrum with  $E_{\text{max}} = 695$  keV is emitted in the decay of  $\text{Te}^{127}$ .<sup>4</sup> The  $\beta$  spectrum with  $E_{\text{max}} = 980$  reported by Hebb<sup>2</sup> was not disclosed by our measurements. The intensities of the partial spectra which we obtained were also somewhat different from that given by Hebb.<sup>2</sup>

### $\beta\gamma$ AND $\gamma e^-$ COINCIDENCES

Measurements of  $\beta\gamma$  and  $\gamma e^-$  coincidences were carried out on an arrangement consisting of a two-lens  $\beta$  spectrometer and a scintillation  $\gamma$  spectrometer connected in a coincidence circuit. This arrangement has already been described in detail.<sup>5,6</sup> In our work, we used a commercial coincidence circuit of type BDS-1, a preamplifier of an improved type, and a new high-voltage stabili-

zer, which kept the supply voltage of the photomultipliers in the  $\beta$  and  $\gamma$  channels constant to within 0.06%. In the  $\gamma$  channel, we used a NaI(Tl) crystal 40 mm in diameter and 40 mm thick. The relative half-width of the  $\text{Cs}^{137}$   $\gamma$  lines was 11%. In the  $\beta$  channel, we used an anthracene crystal 15 mm in diameter and 2 mm thick. The radioactive source had the shape of a circle 8–12 mm in diameter and 2–3 mg/cm<sup>2</sup> thick. The resolving power of the  $\beta$  spectrometer was then  $\sim 4\%$  with a transmission of the order of 2%. All the measurements were carried out with a resolving time of  $2\tau = 7 \times 10^{-8}$  sec. Under these conditions, the relative counting efficiency attained 80%. To separate the partial  $\beta$  spectra, the differential window of the  $\beta$ -channel analyzer was set on the photopeak of the  $\gamma$  line under study and the number of  $\beta\gamma$  coincidences was measured as a function of the energy of the electrons focused by the  $\beta$  spectrometer. From the corresponding Fermi plot, we obtained the values of the maximum energies of the  $\beta$  spectra. In some cases an integral threshold was used in the  $\beta$  channel.

All the obtained results are shown in Table IV. In this table, column 1 lists the energies of the  $\gamma$  lines with which the coincidences were measured. Also shown are the mean values of the maximum energies of the partial spectra which were calculated from the values of the maximum energy obtained in the coincidences with various  $\gamma$  quanta.

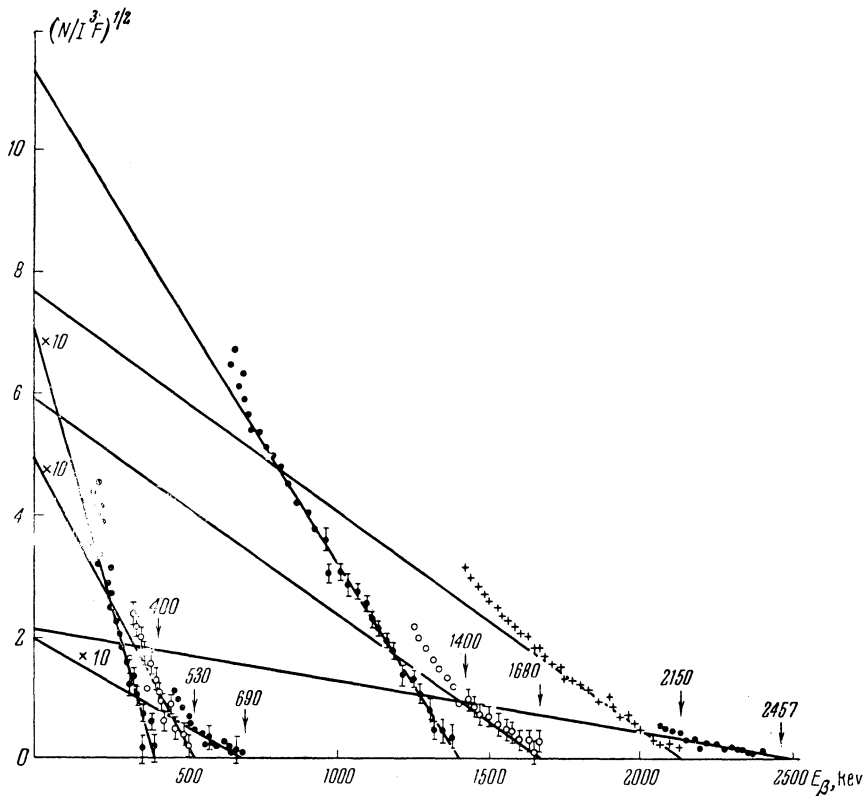


FIG. 3. Fermi plot for  $\beta$  spectrum of  $\text{Te}^{131\text{m}}$ .

**Table IV**  
 $\beta\gamma$  Coincidences of  $\text{Te}^{131}$ 

$E_\gamma$ , keV	$E_{\beta \text{ max}}$ , keV			
780	1350±30	590±30	460±40	225±40
850	1380±40	590±30	420±40	200±40
920		—	535±50	380±40
1140	—	580±50	420±100	220±50
≥1300	—	680±100	425±25	—
≥1900	—	545±30	345±70	—
Mean value of $E_{\beta \text{ max}}$ , keV	1365±25	570±30	420±30	215±15

Shown in Fig. 4a is a Fermi plot for the  $\beta$  spectra in coincidence with 780-keV  $\gamma$  lines; Fig. 4b shows a Fermi plot for  $\beta$  spectra in coincidence with  $\gamma$  quanta whose energy exceeds 1900 keV.

### $\gamma$ RAYS FOLLOWING THE HARD $\beta$ SPECTRA ( $E \geq 600$ KEV)

We presented previously<sup>1</sup> the results of  $\beta\gamma$  coincidence measurements on a scintillation spectrometer. It was then reported that  $\gamma$  rays with energies of 850, 780, 590, 450, 330, and 150 keV were observed in coincidences with  $\gamma$  rays of energy  $\geq 600$  keV. In these measurements, however, the contribution from coincidences was not taken into account. In the present experiment, similar measurements were made, in which this contribution was taken into account. The results are shown in

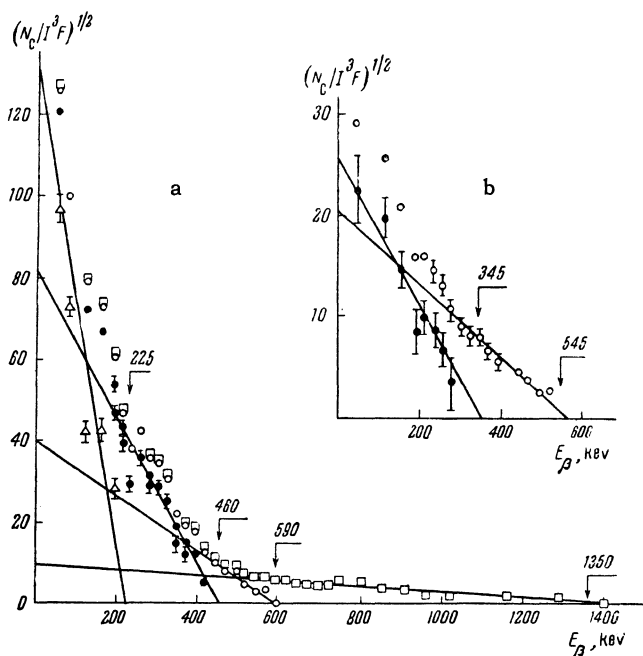


FIG. 4. a—Fermi plot of the spectrum of  $\beta$  particles in coincidence with 780-keV  $\gamma$  rays; b—Fermi plot for coincidences with  $\gamma$  rays  $\geq 1900$  keV. Here and elsewhere  $N_c$  is the coincidence counting rate.

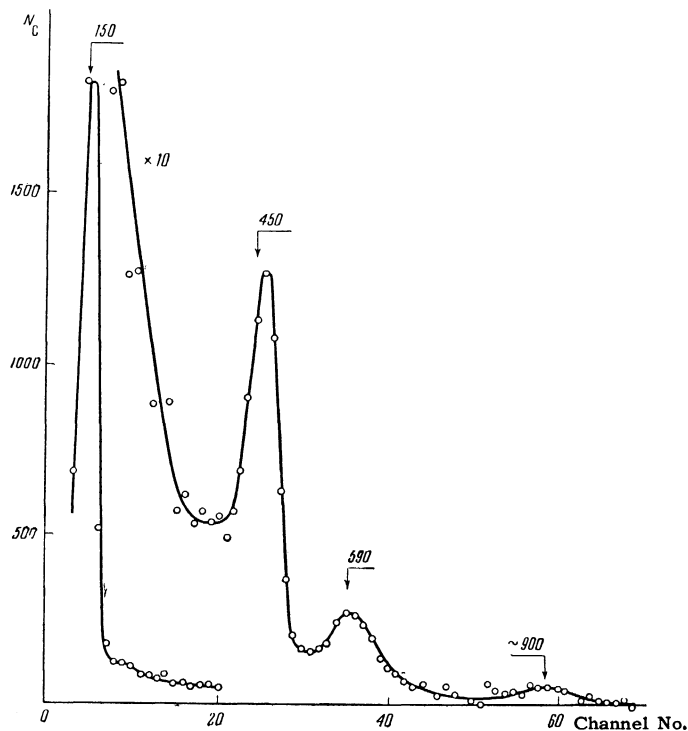


FIG. 5.  $\gamma$ -ray spectrum in coincidence with  $\beta$  electrons of energy  $\geq 600$  keV.

Fig. 5. As seen from the figure, only  $\gamma$  transitions with energies of 150, 450, 590 keV and possibly  $\sim 900$  keV take part in the coincidences. It is evident that all the remaining  $\gamma$  transitions proceed from levels that are populated as a result of soft  $\beta$  spectra.

### $\gamma\gamma$ COINCIDENCES AND CONSTRUCTION OF THE DECAY SCHEME

Shown in Figs. 6 and 7 are the  $\gamma$  spectra obtained in coincidences with the hardest  $\gamma$  rays of  $\text{Te}^{131}$ . Peaks from  $\gamma$  rays of 81 and  $\sim 240$  keV (Fig. 6) stand out in the spectrum of coincidences with all  $\gamma$  rays of energy  $\geq 1800$  keV (i.e., 1920, 2000, and 2240 keV). The absence of a peak from 150-keV  $\gamma$  rays (transition from the first excited level) indicates that all these transitions proceed to the ground state of  $\text{I}^{131}$ . Then it is natural to interpret the 81- and 240-keV  $\gamma$  rays as transitions between the levels 1.92 and 2.0 Mev (80 keV) and 2.0 and 2.24 Mev (240 keV). During the measurements of the spectrum shown in Fig. 7, the window of the control analyzer was set on the peak from the 1650-keV  $\gamma$  rays. In comparison with the spectrum of Fig. 6, there are the additional peaks here from 100- and 330-keV  $\gamma$  rays. In the energy region of 180–260 keV, a plateau is observed. Evidently, apart from the 240-keV peak, there is also a 200-keV  $\gamma$  ray peak. The peak at 150 keV, as shown by an estimate, can largely be explained

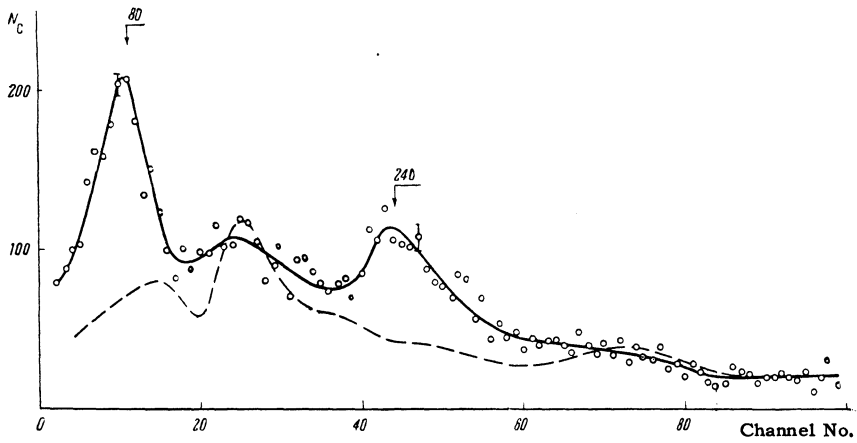


FIG. 6.  $\gamma$  spectrum in coincidence with  $\gamma$  rays of energy  $\geq 1800$  keV. The dotted line indicates the contribution from random coincidences.

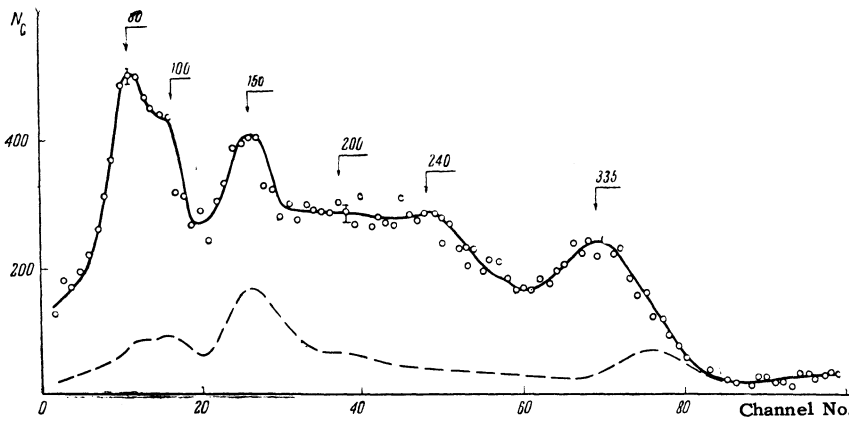


FIG. 7.  $\gamma$  spectrum in coincidence with 1650-keV  $\gamma$  rays. The dotted line indicates the contribution from random coincidences.

by the random-coincidence background. Hence, it is clear that the 1650-keV transition also proceeds to the ground state. Transitions with energies of 100, 200, and 330 keV evidently occur between levels lying in the interval of 1.92 – 1.65 MeV. The energy of the 1650-keV transition was determined to an accuracy of  $\pm 1$  keV. A more accurate value of the energy of the level from which this transition takes place can be obtained from the fact that the 780- and 840-keV  $\gamma$  rays are emitted in cascade. This was demonstrated earlier<sup>1,2</sup> and is confirmed in the present experiment. We thus obtain an energy of  $1.620 \pm 0.015$  MeV for this level.

Furthermore,  $\gamma\gamma$  cascades of 780-1140, 780-1220, and 1140-80 keV were also observed. This indicates that the 1140-keV and 1220-keV transitions proceed from the  $1.920 \pm 0.20$  MeV and  $2.000 \pm 0.20$  MeV levels, respectively. It should be noted that, since the energy of the 81-keV transition is known to an accuracy of  $\pm 0.5$  keV, the difference in the energies of these two levels is determined to the same accuracy. The levels lying in the 1.92 – 1.62 MeV interval were not reliably established by us, since direct transitions from them to the ground state were not observed, and the spectrum of soft  $\gamma$  quanta between them had a quite complex character and could not be reliably inter-

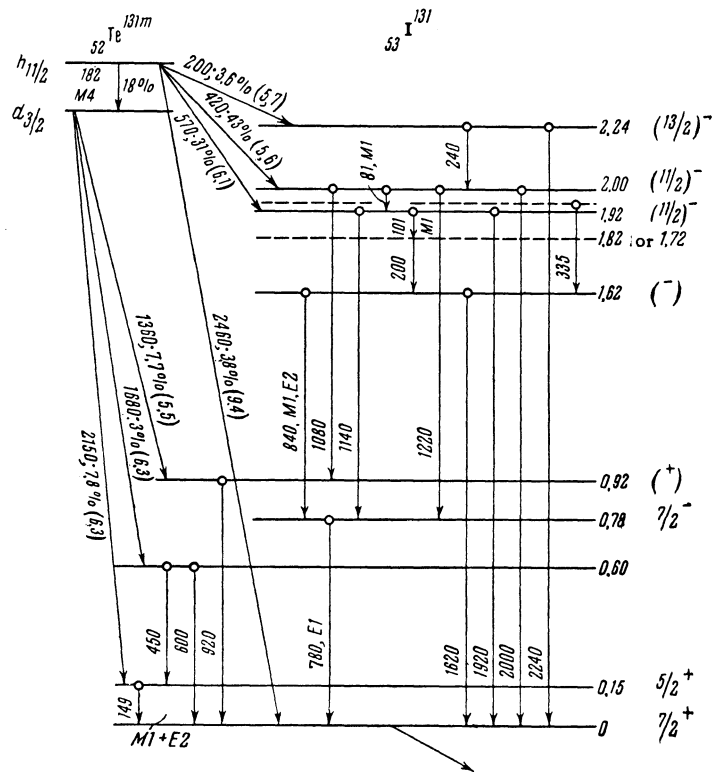


FIG. 8. Decay scheme of  $\text{Te}^{131}$ . The energies of the levels are given in MeV and the energies of the transitions in keV.

puted. Moreover, the energies of the partial  $\beta$  transitions were not determined with sufficient accuracy. We also established the presence of coincidences between 920- and 1080-keV  $\gamma$  rays. The energy of this cascade is 2000 keV, and we therefore assumed that it proceeds from the 2.0 MeV level to the ground state. Since in the resolution of the singles  $\gamma$  spectrum it was found that the intensity of the 920-keV transition is greater than the intensity of the 1080-keV transition (see Table I), then this cascade evidently goes through the 0.920-MeV level and not through the 1.08-MeV level. Moreover, in the spectrum of coincidences with  $\beta$  electrons of energy  $> 600$  keV (Fig. 5) there is an indication of the presence of a peak with energy  $\sim 900$  keV which can be associated with a 920-keV  $\gamma$  transition following the 1360-keV  $\beta$  transition. The position of the levels at 0.15, 0.6, and 0.78 MeV was established by us earlier.<sup>1</sup>

Figure 8 shows the general scheme of the decay of  $\text{Te}^{131}$  nuclei which agrees with the results of the measurements described above.

#### DISCUSSION OF THE DECAY SCHEME. SPINS AND PARITIES OF THE LEVELS

The most intensive  $\beta$  transitions of the  $\text{Te}^{131}$  nucleus are the  $\beta$  transitions of energies 420 and 570 keV proceeding to levels that are close to 2 MeV. From energy considerations they should proceed from the isomeric state  $\text{Te}^{131\text{m}}$  with the characteristic  $11/2^-$ . The values of the quantity  $\log ft$  for  $\beta$  transitions of 420, 570, and 200 keV (see Table III) indicate that these transitions are evidently allowed. Therefore the 2.24-, 2.0-, and 1.92-MeV levels (and also, possibly, other high-lying levels) have high spin values, from  $9/2$  to  $13/2$ , and negative parity. Furthermore, 780-keV level has a negative parity, since the transition from this level to the ground state is of the E1 type. This level is populated almost entirely as a result of the intense  $\gamma$  transitions of 840, 1140, and 1220 keV. The  $\beta$  transitions to this level were not observed either from the isomeric or ground state of  $\text{Te}^{121}$ . This

result can be explained only if the 780-keV level has a spin and parity of  $7/2^-$ . The characteristics of the  $\text{I}^{131}$  levels proposed on the basis of the available experimental data ( $\log ft$  for  $\beta$  transitions, intensities and multipole orders of  $\gamma$  transitions) are also shown in Fig. 8. The ground and first excited states of  $\text{I}^{131}$  are the  $g_{7/2}$  and  $d_{5/2}$  states predicted by the single-particle model given in reference 1. The 600-keV level can also be a single-particle  $d_{3/2}$ . The remaining levels apparently cannot be explained within the framework of the single-particle model.

In conclusion, the authors express their gratitude to M. Radoevich for aid in carrying out the experiments and in the analysis of the experimental data, to S. A. Sergeev for considerable help in setting up the apparatus, and to V. O. Kordyukovich for performing part of the radiometric work.

<sup>1</sup> Bădescu, Mitrofanov, Sorokin, and Shpinel', *Izv. Akad. Nauk SSSR, Ser. Fiz.* **23**, 1434 (1959), Columbia Tech. Transl. p. 1424.

<sup>2</sup> E. Hebb, *Phys. Rev.* **97**, 987 (1955).

<sup>3</sup> A. A. Sorokin, *Izv. Akad. Nauk SSSR, Ser. Fiz.* **23**, 1445 (1959), Columbia Tech. Transl. p. 1434.

<sup>4</sup> B. S. Dzheleпов and L. K. Peker, *Схемы распада радиоактивных ядер (Decay Schemes of Radioactive Nuclei)*, Press of the Acad. Sci. U.S.S.R., 1958.

<sup>5</sup> Delyagin, Sorokin, Forafontov, and Shpinel', *Izv. Akad. Nauk SSSR, Ser. Fiz.* **20**, 913 (1956), Columbia Tech. Transl. p. 828.

<sup>6</sup> Parfenova, Forafontov, and Shpinel', *Izv. Akad. Nauk SSSR, Ser. Fiz.* **21**, 1601 (1957), Columbia Tech. Transl. p. 1590.

<sup>7</sup> L. A. Sliv and I. M. Band, *Таблицы коэффициентов внутренней конверсии на К-оболочке (Table of Internal-Conversion Coefficients for the K-Shell)*, Press of the Acad. Sci. U.S.S.R. 1956.